Article

Immunity

Smad2 and Smad3 Inversely Regulate TGF-β Autoinduction in *Clostridium butyricum*-Activated Dendritic Cells

Graphical Abstract

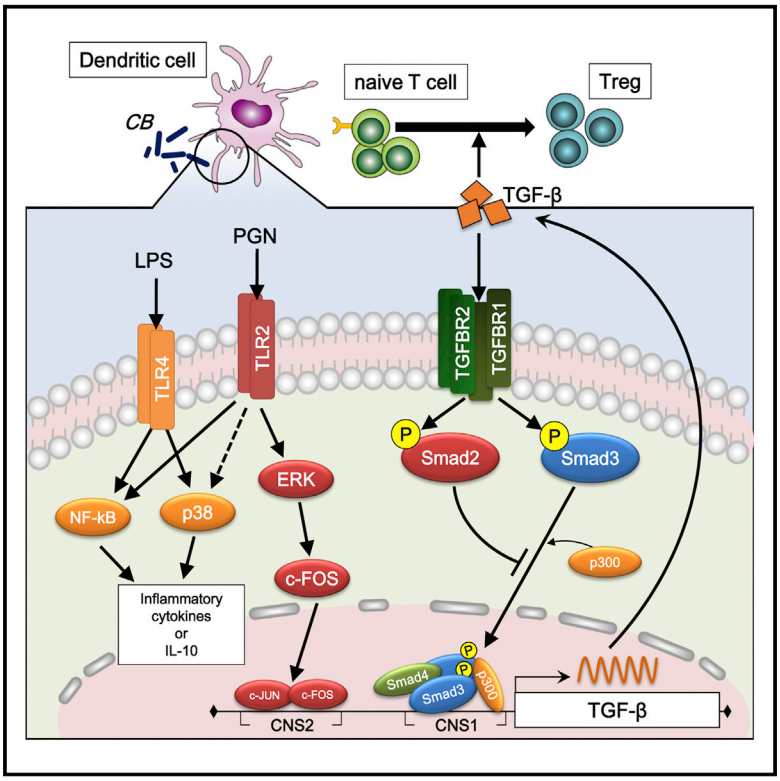

Authors

Ikkou Kashiwagi, Rimpei Morita, Takashi Schichita, ..., Atsushi Hayashi, Takanori Kanai, Akihiko Yoshimura

Correspondence

yoshimura@a6.keio.jp

In Brief

Clostridium species have been shown to induce accumulation of induced regulatory T cells in the colon. Yoshimura and colleagues demonstrate that induction of intestinal regulatory T cells is dependent on TGF-β1 from lamina propria dendritic cells, and TGF-β1 is induced through a cooperation between TLR2-AP-1 and TGF-β-Smad signaling pathways.

Highlights

- *Clostridium butyricum* promotes iTreg cell generation through induction of TGF-β from DCs
- *C. butyricum*-mediated TGF-β1 induction in DCs is dependent on the TLR-ERK-AP1 pathway
- Autocrine TGF-β-Smad3 signal is necessary for robust TGF-β expression in DCs
- Smad2 negatively regulates TGF-β expression, and Smad2-deficient DCs are tolerogenic

Kashiwagi et al., 2015, Immunity *43*, 65–79
July 21, 2015
http://dx.doi.org/10.1016/j.immuni.2015.06.010

Immunity
Article

Smad2 and Smad3 Inversely Regulate TGF-β Autoinduction in *Clostridium butyricum*-Activated Dendritic Cells

Ikkou Kashiwagi,[1] Rimpei Morita,[1] Takashi Schichita,[1,2] Kyoko Komai,[1] Keita Saeki,[1] Makoto Matsumoto,[3] Kiyoshi Takeda,[4] Masatoshi Nomura,[5] Atsushi Hayashi,[6,7] Takanori Kanai,[6] and Akihiko Yoshimura[1,*]
[1]Department of Microbiology and Immunology, Department of Internal Medicine, Keio University School of Medicine, Tokyo 160-8582, Japan, and Japan Science and Technology Agency, CREST, Tokyo 102-0076, Japan
[2]PRESTO (Precursory Research for Embryonic Science and Technology), Chiyoda-ku, Tokyo 102-0075, Japan
[3]Department of Immunology and Medical Zoology, Hyogo College of Medicine, 1-1 Mukogawa-cho, Nishinomiya, 663-8501, Japan
[4]Laboratory of Immune Regulation, Department of Microbiology and Immunology, Graduate School of Medicine, WPI Immunology Frontier Research Center, Osaka University, Suita, Osaka 565-0871, Japan
[5]Graduate School of Medical Sciences, Kyushu University, Fukuoka 812-8582, Japan
[6]Division of Gastroenterology and Hepatology, Department of Internal Medicine, Keio University School of Medicine, Tokyo 160-8582, Japan, and Japan Science and Technology Agency, CREST, Tokyo 102-0076, Japan
[7]Miyarisan Pharmaceutical Co., Ltd., Research Laboratory, Tokyo 114-0016, Japan
*Correspondence: yoshimura@a6.keio.jp
http://dx.doi.org/10.1016/j.immuni.2015.06.010

SUMMARY

Colonization with a mixture of *Clostridium* species has been shown to induce accumulation of induced regulatory T (iTreg) cells in the colon. Transforming growth factor-β (TGF-β) is an essential factor for iTreg cell induction; however, the relationship between *Clostridium* species and TGF-β remains to be clarified. Here we demonstrated that a gram-positive probiotic bacterial strain, *Clostridium butyricum* (*C. butyricum*), promoted iTreg cell generation in the intestine through induction of TGF-β1 from lamina propria dendritic cells (LPDCs). *C. butyricum*-mediated TGF-β1 induction was mainly Toll-like receptor 2 (TLR2) dependent, and the ERK-AP-1 kinase pathway played an important role. In addition, the autocrine TGF-β-Smad3 transcription factor signal was necessary for robust TGF-β expression in DCs, whereas Smad2 negatively regulated TGF-β expression. Smad2-deficient DCs expressed higher concentrations of TGF-β and were tolerogenic for colitis models. This study reveals a novel mechanism of TGF-β induction by *Clostridia* through a cooperation between TLR2-AP-1 and TGF-β-Smad signaling pathways.

INTRODUCTION

Intestinal microbiota contribute to many host physiological processes, including nutrient acquisition and development of the gut-specific immune system, as well as protection from infectious pathogens (Hill and Artis, 2010; Hooper et al., 2012). Recent advances in the field of mucosal immunology have uncovered several roles of intestinal microbiota in the establishment of interleukin-17 (IL-17)-producing helper T (Th17) cells and regulatory T (Treg) cells (Ivanov and Honda, 2012). A complex mixture of 46 strains of *Clostridium* has been shown to promote the subsequent accumulation of IL-10-producing iTreg cells in mice, which suppresses colitis in a dextran sodium sulfate (DSS) colitis model (Atarashi et al., 2011). The same group also identified the 17 strains of clusters IV, XIVa, and XVIII of *Clostridia* from the human indigenous microbiota that provide bacterial antigens and a transforming growth factor β (TGF-β)-rich environment to help expansion and differentiation of iTreg cells (Atarashi et al., 2013).

The molecular mechanism of iTreg cell induction by *Clostridia* remains to be clarified. At present, it has been well established that TGF-β and its downstream transcription factors Smad2 and Smad3 are essential for iTreg cell generation (Chen et al., 2003; Takimoto et al., 2010). Atarashi et al. (2011, 2013) has shown that *Clostridium* species induce TGF-β from epithelial cells. On the other hand, several groups have shown that microbial metabolites such as a short-chain fatty acid, butyrate, facilitate iTreg cell generation (Arpaia et al., 2013; Furusawa et al., 2013). Butyrate could inhibit histone deacetylase (HDAC), resulting in enhanced histone H3 acetylation in the promoter and conserved non-coding sequence (CNS) regions of the Foxp3 locus. However, butyrate alone does not induce iTreg cells, and TGF-β is still essential for iTreg cell development even in the presence of butyrate.

Although TGF-β is produced by a large variety of cells in the intestinal mucosa, including intestinal epithelial cells, lymphocytes, macrophages, and dendritic cells (DCs), the source of TGF-β for iTreg cell generation in the intestine has not been determined. Several reports indicate that a population of $CD103^+$ DCs in mesenteric lymph nodes (mLNs) is important for the development of iTreg cells in a retinoic acid (RA)-dependent manner (Coombes and Powrie, 2008). Another report shows that LPDCs in the small intestine possess a higher potential to generate iTreg cells than lymphoid organ-derived DCs (Sun et al., 2007). Although it is not clear where iTreg cells are developed, $CD103^+$ DCs in the intestine are now widely believed

to induce iTreg cells by providing antigens, RA, and TGF-β (Benson et al., 2007; Coombes et al., 2007; Ruane and Lavelle, 2011). In addition, TGF-β signals inside DCs are also necessary for proper Foxp3$^+$ T cell development: DC-specific disruption of TGF-β receptor II shows abnormal Treg cell phenotypes (Ramalingam et al., 2012). However, the function of the TGF-β signal in DCs for Treg cell development has not been clarified.

Clostridium butyricum (*C. butyricum*) is classified in *Clostridium* cluster I and is a group member of allochthonous bacteria (Sato and Tanaka, 1997). *C. butyricum* has been used as a probiotic in clinical practice (Seki et al., 2003), and we have demonstrated that administration of the probiotic bacterial strain *C. butyricum* prevents experimental colitis (Hayashi et al., 2013). We have shown that depletion of Treg cells by anti-CD25 Ab overrides the protective effect of *C. butyricum*, raising a possibility that *C. butyricum* affects Treg cell development (Hayashi et al., 2013).

In the present study, we demonstrate that *C. butyricum* promoted iTreg cell generation by inducing large amounts of TGF-β from DCs both in vivo and in vitro. Induction of TGF-β was toll-like receptor-2 (TLR2) dependent, and the ERK-AP-1 kinase pathway played an important role for TGF-β promoter activation. We also identified an autoinduction mechanism of TGF-β production in which Smad3 directly activated the *Tgfb1* promoter. Smad2 had an opposite function that inhibited the *Tgfb1* promoter activation. Consistent with this observation, *Smad2*-deficient bone-marrow-derived DCs (BMDCs) induced more iTreg cells than wild-type (WT) BMDCs, and adoptive transfer of *Smad2*$^{-/-}$ DCs ameliorated experimental colitis. This study revealed the importance of the autoinduction mechanism of TGF-β for efficient iTreg cell generation and immune tolerance by DCs.

RESULTS

C. butyricum Suppresses Experimental Colitis by a TGF-β-Dependent Mechanism

To investigate the relationship among *C. butyricum*, TGF-β, and iTreg cells, we performed a DSS-induced acute colitis model after treatment of mice with *C. butyricum* spore. Consistent with the previous report (Hayashi et al., 2013), *C. butyricum* administration reduced the severity of DSS-induced colitis as judged from body weight loss and colon length (Figure 1A). *C. butyricum* administration reduced the expression of inflammatory cytokines including interleukin-12 p40 (IL-12p40), tumor necrosis factor-α (TNF-α), and IL-6, but increased IL-10 and TGF-β1, in colonic lamina propria DCs (LPDCs) on day 8 after DSS treatment (Figure 1B). Because *Tgfb2* and *Tgfb3* mRNA amounts were much lower (<2%) than *Tgfb1* (Figure 1B), we used TGF-β as TGF-β1 hereafter unless otherwise noted.

To confirm the protective role of TGF-β in the DSS-induced colitis model, we treated mice with anti-TGF-β antibody (Ab). Anti-TGF-β Ab abrogated the protective effect of *C. butyricum* on colitis (Figure 1A) and the suppressive effect on the inflammatory cytokine expression in LPDCs (Figure 1B). Anti-TGF-β Ab had little effect on IL-10, whereas *Tgfb1* expression in DCs was reduced by anti-TGF-β Ab treatment (Figure 1B). Interferon-γ (IFN-γ) expression in CD4$^+$ T cells was enhanced by DSS treatment, which was reduced by *C. butyricum* administration. This protective effect of *C. butyricum* was also reverted by anti-TGF-β-Ab (Figure S1A). *C. butyricum* exhibited a reduced T helper 1 (Th1) cell induction potential compared with *E. coli* or *Enterococcus faecalis* in mixed lymphocyte reaction (MLR) in vitro (Figures S1B and S1C). These data suggest that the anti-inflammatory effect of *C. butyricum* against DSS-induced colitis is associated with TGF-β-dependent reduction of IFN-γ expression.

We then examined the effect of *C. butyricum* and TGF-β on iTreg cell development. As reported previously (Atarashi et al., 2011), approximately 60%–70% of Foxp3$^+$CD4$^+$ Treg cells in the colon were Helios negative, i.e., they were iTreg cells (Figures 1C and 1E). After *C. butyricum* administration for 2 weeks, the fraction of Foxp3$^+$ cells among CD4$^+$ T cells increased 2-fold (Figures 1C and 1D), which was mostly due to the increase of Helios$^-$ iTreg cells (Figures 1C and 1E). Anti-TGF-β Ab abrogated the effect of *C. butyricum* on the increase of iTreg cells (Figures 1C and 1D) and partly reduced Helios$^-$ iTreg cells (Figure 1E). These data indicate that *C. butyricum* promotes the development of iTreg cells in the colon by enhancing TGF-β expression.

To determine which cells (epithelial cells or DCs) are important source of TGF-β for iTreg cell induction, we compared *Tgfb1* mRNA contents in EpCAM$^+$ epithelial cells and CD11c$^+$ LPDCs. As shown in Figure 1F, *Tgfb1* mRNA amounts per cell were much higher in LPDCs than in epithelial cells in vivo. In addition, the response to *C. butyricum* was also greater in LPDCs than in epithelial cells (Figure 1F). Depletion of DCs by using *Itgax*-DTR mice (Ohnmacht et al., 2009) resulted in the reduction of TGF-β and Foxp3 expression in the whole intestine (Figures S1D and S1E). To clarify which cells in the LPDC fraction produce TGF-β, we separated CD11c$^+$MHC-II^{hi} cells by CD103 and CX_3CR1 expression (Varol et al., 2009). CD103$^+$$CX_3CR1^-$ DCs expressed the highest amount of TGF-β in response to *C. butyricum* administration in vivo (Figure S1F). These data are consistent with previous reports indicating that CD103$^+$ DCs are most important for iTreg cell induction (Coombes et al., 2007; Sun et al., 2007; Worthington et al., 2011).

TLR Signals Promote TGF-β Production in DCs

We noticed that the protective effect against DSS-induced colitis was observed even when heat-killed *C. butyricum* was administered (Figure S2), suggesting that components of *C. butyricum* were probably sufficient to induce TGF-β. Therefore, we first measured TGF-β expression in vitro from isolated LPDCs in response to major TLR ligands (Figure 2A). Epithelial cells were used as a control. Similar to *C. butyricum*, both LPS (lipopolysaccharide, a TLR4 ligand) and PGN (peptidoglycan, a TLR2 ligand) induced *Tgfb1* expression in primary LPDCs; however, PGN showed a stronger effect than LPS (Figure 2A). Although epithelial cells responded to PGN, the response was much weaker than that of LPDCs (Figure 2A).

Next, we asked whether BMDCs exhibit a TGF-β production similar to LPDCs in response to bacteria and TLR ligands. TGF-β protein concentration was measured with a reporter cell line, MFB-F11, by which both total and biologically active forms of TGF-β can be detected with extremely high sensitivity (Matsumura et al., 2007). As shown in Figure 2B, BMDCs secreted TGF-β at high concentrations in response to heat-killed bacteria (*C. butyricum* and *E. coli*) *and* TLR ligands (LPS and PGN),

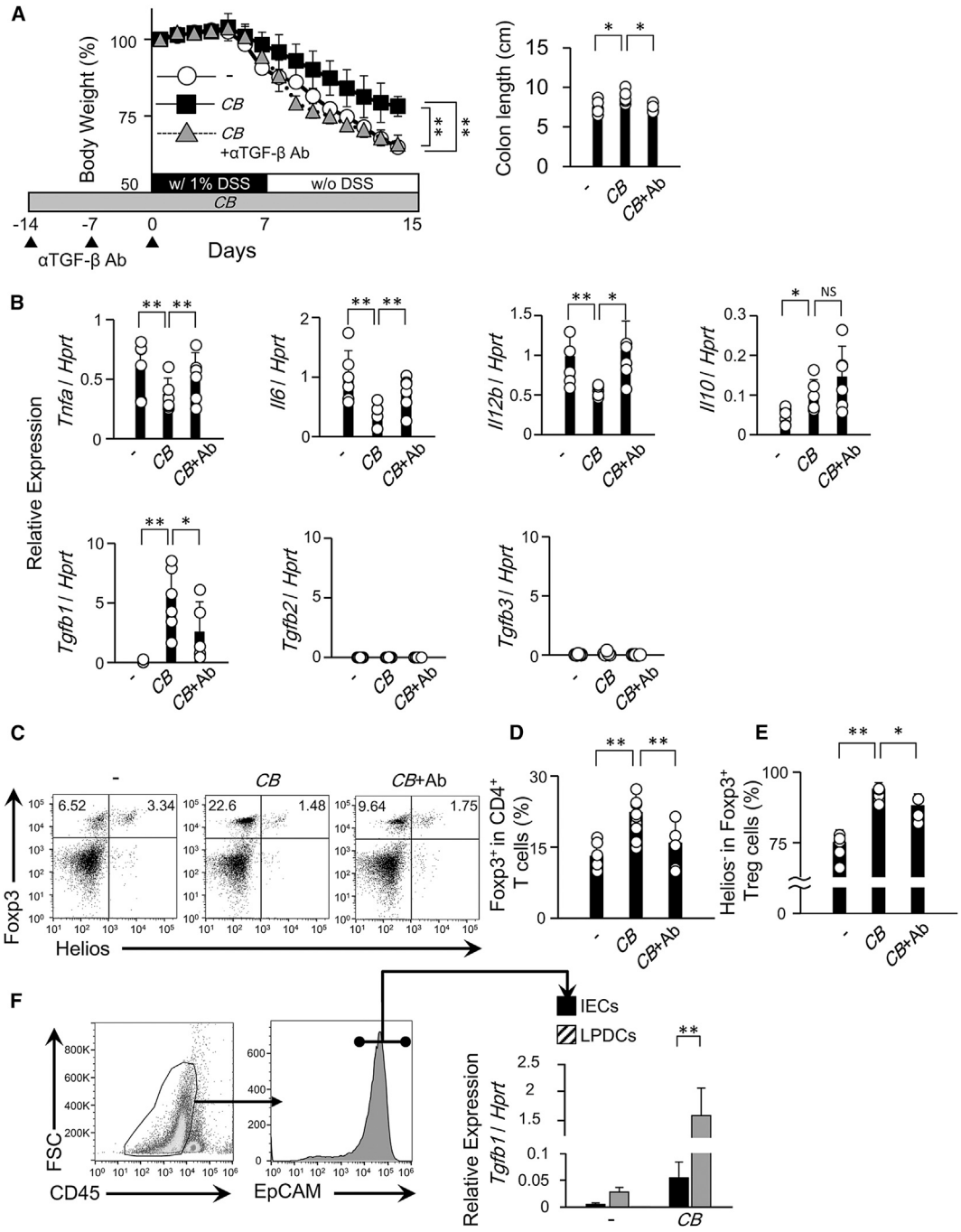

Figure 1. *Clostridium butyricum* Promotes TGF-β-Dependent iTreg Cell Development in the Lamina Propria and Suppresses Acute DSS-Induced Colitis

(A) Body weight changes of mice administered with *C. butyricum* (CB) with or without anti-TGF-β Ab (Ab) during DSS-induced colitis. Colon length on day 8 was also measured (right). C57BL/6 mice were fed with a normal diet (−) or a diet containing *C. butyricum* for 2 weeks. Neutralizing anti-TGF-β Ab was intraperitoneally injected on days −14, −7, and 0 of DSS treatment.

(B) Quantitative RT-PCR (qRT-PCR) analysis of cytokine mRNA amounts in CD11c$^+$ DCs isolated from colonic LPDCs on day 8 after DSS treatment. Expression is normalized to *Hprt*. Each circle represents an individual animal.

(C–E) Mice were administered *C. butyricum* with or without anti-TGF-β Ab for 2 weeks. LP mononuclear cells were isolated from colonic LP and stained with anti-CD4, anti-Foxp3, and anti-Helios antibodies. The percentage of Foxp3$^+$ within the CD4$^+$ cells (D) and the percentage of Helios$^-$ cells within the Foxp3$^+$ cells (E) in the colonic LP of the indicated mice are shown.

(F) Comparison of *Tgfb1* mRNA amounts in CD45$^-$EpCAM$^+$ intestinal epithelial cells (IECs) and CD11c$^+$ LPDCs in mice fed with or without *C. butyricum*. FACS profiles of IECs are shown in the right panel. *Tgfb1* mRNA content was measured by qRT-PCR.

All data represent the mean ± SEM (n ≥ 5 mice group). *p < 0.05, **p < 0.01. Data were pooled from two independent experiments. See also Figure S1.

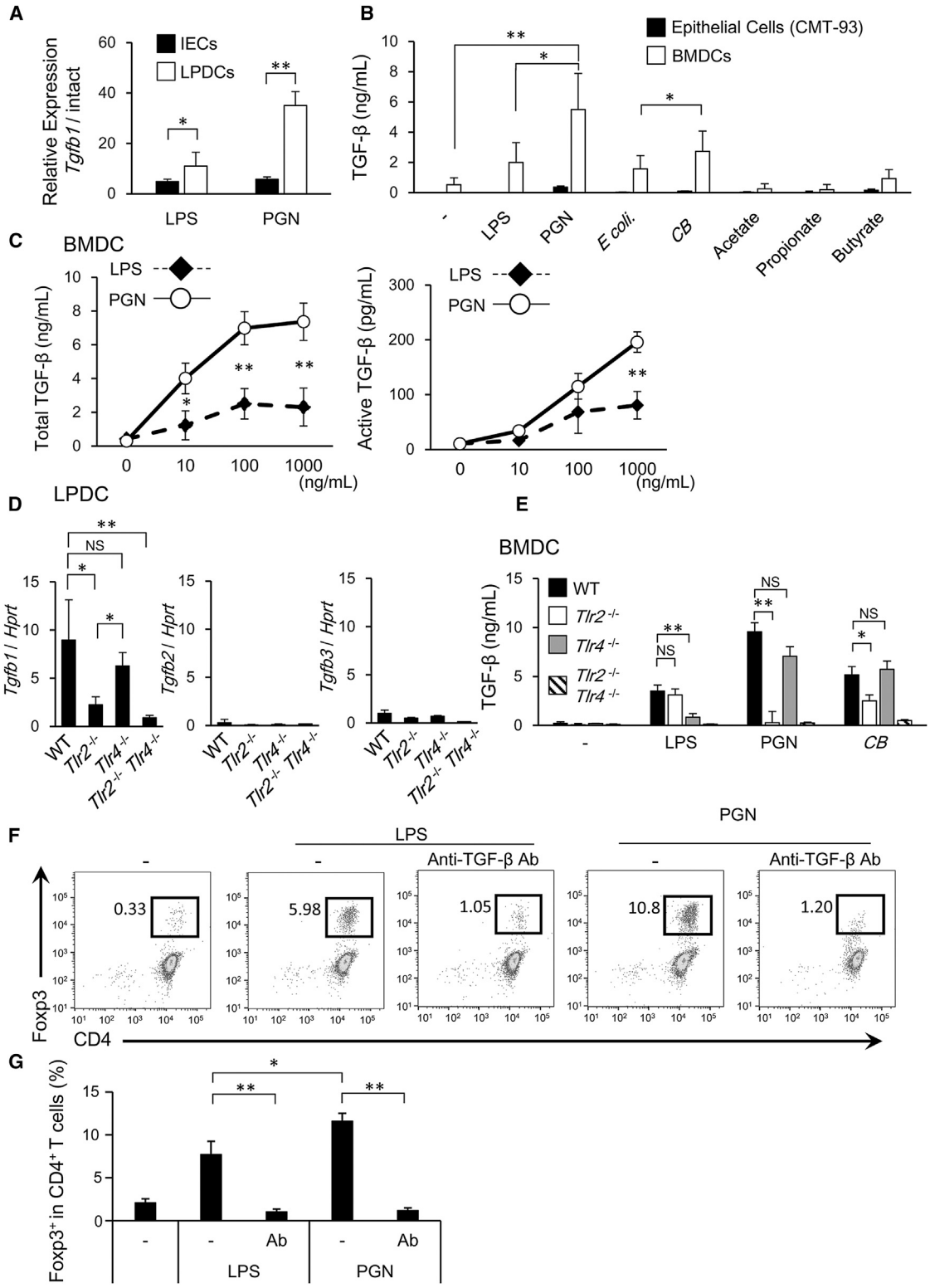

Figure 2. TLR2-Dependent TGF-β Production from DCs

(A) *Tgfb1* mRNA expression in CD45$^-$EpCAM$^+$ IELs and CD11c$^+$ LPDCs form normal-diet mice stimulated with or without 100 ng/ml LPS or 100 ng/ml PGN for 3 hr. Relative *Tgfb1* mRNA contents (fold increase) are shown compared with those without stimulation.

(B) TGF-β amounts from CMT-93 cells and BMDCs (1 × 10^6) stimulated with the indicated materials for 24 hr. Total TGF-β concentrations in the culture supernatant were measured by the SEAP assay.

(legend continued on next page)

compared with the colonic epithelial cell line CMT-93. Heat-killed *C. butyricum* also induced TGF-β production from BMDCs more strongly than did *E. coli* (Figure 2B). Short chain fatty acids, which have been shown to facilitate Foxp3 transcription factor expression in iTreg cells, had little effect on TGF-β production. Similar to LPDCs, *Tgfb2* and *Tgfb3* expression was much lower compared to *Tgfb1* in stimulated BMDCs (data not shown). LPS and PGN dose dependently induced both total and bioactive TGF-β expression in BMDCs. Like LPDCs (Figure 2A), PGN induced higher amount of TGF-β compared with LPS in BMDCs (Figure 2C). Although only a small fraction was converted to the bioactive form by BMDCs, PGN was always two to three times more effective than LPS on bioactive TGF-β expression (Figure 2C). These data suggest that TLR2 ligand stimulates TGF-β production more preferentially compared with the TLR4 ligand both in LPDCs and BMDCs.

To confirm that *C. butyricum* induced TGF-β mainly through TLR2 in vivo, we compared *Tgfb* expression in LPDCs from *Tlr2*$^{-/-}$, *Tlr4*$^{-/-}$, and *Tlr2*$^{-/-}$*Ttlr4*$^{-/-}$ mice treated with *C. butyricum*. As shown in Figure 2D, *Tgfb1* expression in LPDCs in vivo depended strongly on TLR2 and weakly on TLR4. Again, *Tgfb2* and *Tgfb3* were much lower than *Tgfb1*. Induction of TGF-β by *C. butyricum* was severely impaired in *Tlr2*$^{-/-}$*Tlr4*$^{-/-}$ mice (Figure 2D). Similarly, TGF-β production from BMDCs stimulated with *C. butyricum* in vitro was almost completely abolished by both TLR2 and TLR4 deficiency; however, TLR2 deficiency showed more profound effect than TLR4 (Figure 2E). These data indicated that *C. butyricum* utilized both TLR2 and TLR4 to induce TGF-β, but the contribution of TLR2 was much greater than that of TLR4.

To demonstrate that TLR2-mediated TGF-β from DCs is important for iTreg cell generation, naive CD4$^+$ T cells from BALB/c mice were co-cultured with LPS- or PGN-primed BMDCs from C57BL/6 mice (Figures 2F and 2G). PGN enhanced the ability of BMDCs to induce Foxp3$^+$ iTreg cells more potently than did LPS. Anti-TGF-β Ab completely abolished the induction of iTreg cells by BMDCs. These data indicate that TLR2 signal-mediated TGF-β production in DCs plays a role in iTreg cell induction.

The ERK-AP-1 Pathway Promotes TGF-β Expression in DCs

We screened chemical inhibitors to examine the mechanism that induces TGF-β expression downstream of TLR2. Major TLR signaling pathways are the IKK-NF-κB pathway, p38, JNK and ERK MAP kinases, and the GSK3β-CREB pathway. Among inhibitors of these pathways, the MEK inhibitor U0126 most strongly reduced the expression of TGF-β from PGN-stimulated BMDCs (Figure 3A, MEKi). Because U0126 suppresses the ERK-AP-1 pathway and AP-1 has been shown to be involved in TGF-β promoter activation (Birchenall-Roberts et al., 1990), we focused on ERK and AP-1. Several reports have suggested that the ERK-AP-1 pathway is differentially activated by TLR2 and TLR4 (Agrawal et al., 2003; Re and Strominger, 2001). Therefore, we examined the activation kinetics of MAP kinases via immunoblotting. PGN more strongly activated ERK and induced c-Fos than LPS did (Figure 3B). c-Jun, a partner of c-Fos, was constitutively expressed regardless of the stimulation.

Next, we analyzed the *Tgfb1* promoter to examine whether AP-1 is directly involved in *Tgfb1* induction. The non-coding region of the *Tgfb1* promoter upstream of exon 1 (−265 to −1; putative CNS1) and a distal region (−1783 to −1273; putative CNS2) were highly conserved among species (Figure 3C). *Tgfb1* promoter reporter constructs (Kinjyo et al., 2006) were transfected into HEK293T cells expressing TLR2, then stimulated with PGN. The reporter assay revealed that the CNS2 region contained PGN-responsive elements, where one AP-1 binding sequence (5′-TGAGTCA-3′; −1403 to −1397) exists (Figure 3D). TLR2-mediated recruitment of AP-1 to this site was confirmed by chromatin immunoprecipitation (ChIP) assay with anti-c-Fos and anti-c-Jun antibodies (Figure 3E). Both c-Fos and c-Jun proteins were recruited specifically to this site after stimulation with PGN in BMDCs. Recruitment of AP-1 to this site was much more intense by PGN stimulation than by LPS stimulation (Figure 3E). Accordingly, transcriptionally active histone modifications such as histone H3 and H4 acetylation (AcH3 and AcH4) and H3 lysine 4 trimethylation (H3K4me3) were strongly enhanced by PGN in this AP-1 region, whereas repressive histone modification, such as H3K27me3 and H3K9m3, were not affected (Figure 3E, AcH3 and Figure S3A). These data indicate that the TLR2-ERK signal recruits AP-1 to CNS2 and induce active histone modifications in the *Tgfb1* promoter.

Next we used DC-specific *Fos*$^{-/-}$ (*Fos*$^{\Delta DC/\Delta DC}$) mice (Figures 3F–3I). PGN-mediated TGF-β protein production was significantly reduced in *Fos*$^{\Delta/\Delta}$ BMDCs (Figure 3F), and active histone modifications of the AP-1 binding region were not induced, while repressive modifications were increased, in *Fos*$^{\Delta/\Delta}$ BMDCs (Figures 3G and S3B). TGF-β mRNA expression was severely reduced in LPDCs from *Fos*$^{\Delta DC/\Delta DC}$ mice compared with WT mice (Figure 3H). In the colon, iTreg and nTreg cells were distinguished by Neuropilin-1 (Nrp1) expression (Figure S3C; Yadav et al., 2012). Consistently, Foxp3$^+$ fraction in CD4$^+$ T cells as well as Nrp1$^-$ iTreg cell fraction were reduced in *Fos*$^{\Delta DC/\Delta DC}$ mice (Figure 3I). Our data suggest that AP-1 activated by the TLR2-ERK pathway plays an essential role in both TGF-β induction in DCs and iTreg cell generation in vivo.

(C) Dose response to LPS and PGN for total (left) and active (right) TGF-β production from BMDCs stimulated with the indicated concentrations of LPS or PGN for 24 hr. Active TGF-β was measured without acid treatment. Data were pooled from three independent experiments.

(D) mRNA contents of TGF-β family genes in LPDCs isolated from *Tlr2*$^{-/-}$, *Tlr4*$^{-/-}$, and *Tlr2*$^{-/-}$*Ttlr4*$^{-/-}$ mice treated with *C. butyricum* for 2 weeks (n = 3–5).

(E) WT, *Tlr2*$^{-/-}$, and *Tlr4*$^{-/-}$ BMDCs were treated with respective stimulation for 24 hr, and total TGF-β in the culture supernatant was measured by the SEAP assay.

(F and G) C57BL/6 BMDCs were primed with LPS or PGN for 24 hr, then co-cultured with CD4$^+$CD62L$^+$ naive T cells from BALB/c mice for 3 days in the presence or absence of anti-TGF-β Ab. Foxp3$^+$ and CD4$^+$ cells were analyzed by flow cytometry. Representative flow cytometry data are shown in (F) and quantitative data of the percentage of Foxp3$^+$ cells among CD4$^+$ T cells are shown in (G).

Data represent the mean ± SEM (n = 3). *p < 0.05, **p < 0.01. Data are representative of three independent experiments. See also Figure S2.

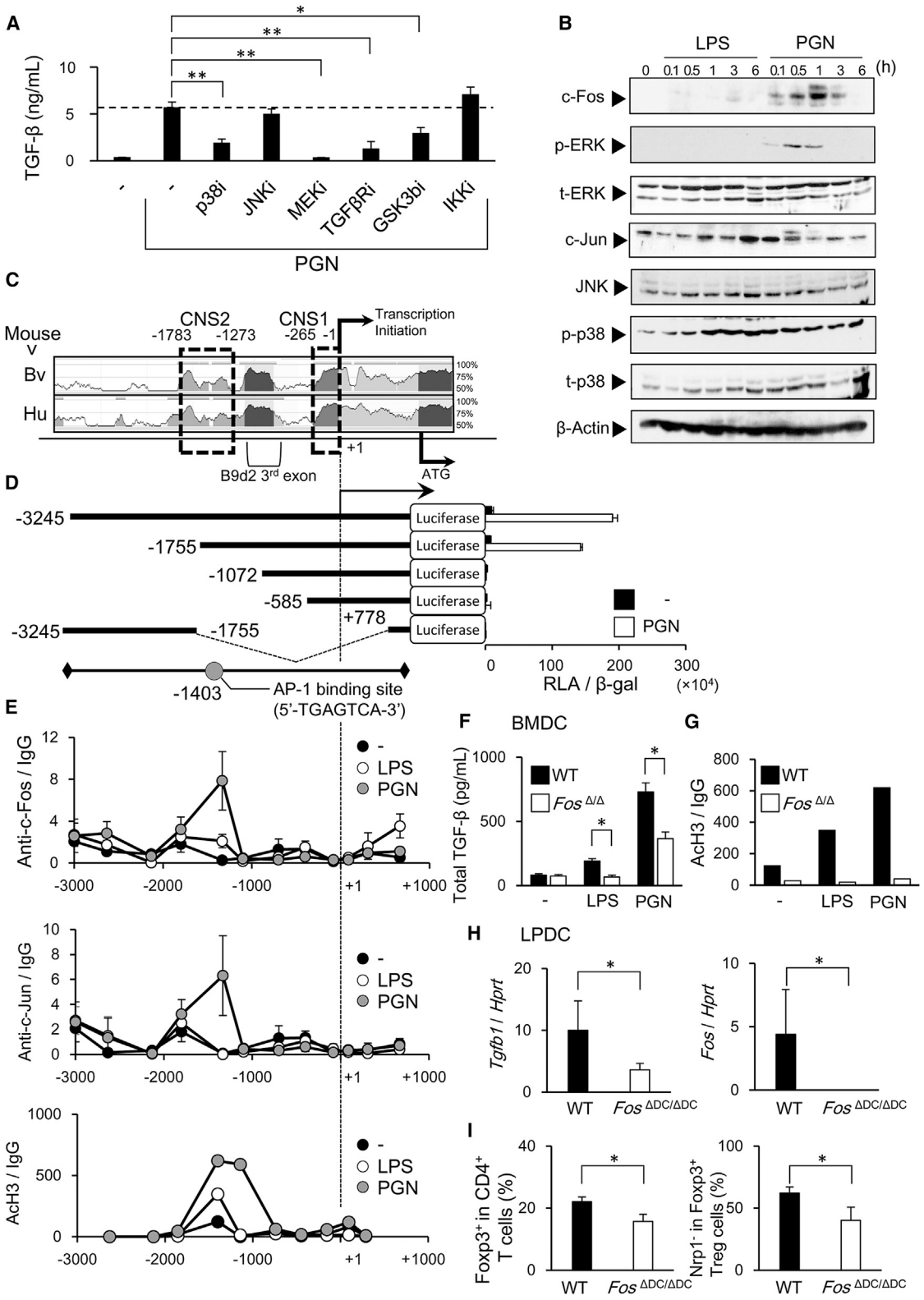

Figure 3. AP-1 Plays an Important Role in TLR-Mediated TGF-β Expression

(A) BMDCs were cultured with the indicated inhibitors for 2 hr before and during treatment with 100 ng/ml PGN for 24 hr. TGF-β in the culture supernatant was measured by SEAP assay.

(B) Immunoblotting of signaling molecules in BMDCs treated with LPS or PGN. BMDCs were stimulated with 10 ng/ml LPS or PGN for the indicated periods.

(legend continued on next page)

Autoinduction of TGF-β Is Mediated by Smad3 and Repressed by Smad2

Chemical inhibitor screening revealed that the TGF-β receptor I kinase inhibitor (TGFβRIi) also strongly suppressed TGF-β production from DCs (Figure 3A). Although autocrine induction (autoinduction) of TGF-β is known in tumor cells (Kim et al., 1990), the significance of this process in DCs has not been investigated. We confirmed that exogenous TGF-β induced TGF-β mRNA transcription both in BMDCs and LPDCs (Figure S4A). Because Smad2 and Smad3 are the major downstream transcription factors of the TGF-β signaling, we examined the involvement of these Smads in autoinduction of TGF-β by using Smad2- and Smad3-deficient BMDCs. Smad2 was specifically deleted in DCs by crossing *Itgax-cre* mice with *Smad2*$^{flox/flox}$ (*Smad2*$^{\Delta DC/\Delta DC}$) mice (Figures S4B and S4C).

As shown in Figures 4A and 4B, Smad3-deficient BMDCs produced extremely low TGF-β protein and *Tgfb1* mRNA in response to PGN or *C. butyricum*. On the other hand, *Smad2*$^{\Delta/\Delta}$ BMDCs produced two times higher concentrations of TGF-β compared with WT BMDCs. Similar positive and negative effects of Smad2 and Smad3 deficiency on TGF-β protein secretion was confirmed in BMDCs stimulated with LPS and *E. coli* (Figure S4D). We next stimulated BMDCs with exogenous TGF-β to show autoinduction of TGF-β. Much lower amounts of *Tgfb1* mRNA were detected in *Smad3*$^{-/-}$ BMDCs stimulated with TGF-β compared with WT BMDCs, whereas higher induction of *Tgfb1* mRNA in *Smad2*$^{\Delta/\Delta}$ BMDCs were observed (Figure 4B). Similarly, *Tgfb1* expression was much higher in LPDCs from *Smad2*$^{\Delta DC/\Delta DC}$ mice than in those from WT mice, whereas LPDCs from *Smad3*$^{-/-}$ mice poorly responded to PGN and TGF-β (Figure 4C).

Next we compared iTreg cell induction potential by BMDCs in vitro. *Smad3*$^{-/-}$ BMDCs primed with either PGN induced lower fraction of iTreg cells than WT BMDCs by allogenic MLR, whereas *Smad2*$^{\Delta/\Delta}$ BMDCs induced higher fraction of iTreg cells (Figures 4D and 4E). This enhanced iTreg cell generation induced by *Smad2*$^{\Delta/\Delta}$ DCs was dependent on endogenous TGF-β, as shown by the fact that TGF-β-neutralizing Ab severely reduced iTreg cell generation (Figure S4E). These data indicate that Smad3 transmits the TGF-β receptor signal that is essential for TGF-β autoinduction and iTreg cell generation, whereas Smad2 negatively regulates these processes.

To confirm the respective positive and negative effects of Smad3 and Smad2 for TGF-β autoinduction, we transduced Smad2 and Smad3 cDNA into BMDCs by using retrovirus, and BMDCs were stimulated with PGN or TGF-β. Forced expression of Smad3 resulted in higher production of TGF-β in response to PGN or TGF-β compared with control BMDCs, whereas Smad2 expression suppressed TGF-β induction (Figure 4F). Forced expression of Smad3 resulted in spontaneous TGF-β expression in BMDCs without any stimulation. Thus, we concluded that Smad3 transmits positive signals, whereas Smad2 transmits negative signals for TGF-β production in BMDCs.

Smad3 Induces Active Histone Modifications of the TGF-β Promoter

Next, we investigated the mechanisms for opposite regulation of TGF-β expression by Smad2 and Smad3. Smad3 regulates transcription of target genes through direct binding to the Smad-binding element (SBE) (Massagué et al., 2005). TGF-β promoter reporter assay via HEK293T cells revealed that Smad3 directly enhanced *Tgfb1* promoter activity in vitro whereas Smad2 did not. Deletion mutant experiments suggested that a Smad3-responsive region was included within 585 bp upstream region of the promoter (Figure 5A). This region contains the CNS1 (−265 to −1), which is adjacent to exon 1 and highly conserved among species (Figure 3C), and there are a number of SBE core sequences (5′-AGAC-3′) (Figure 5A). We then searched the actual Smad binding sites in the promoter in BDMCs stimulated with TGF-β via a ChIP assay. Both Smad2 and Smad3 bound to the SBE-rich CNS1 region around the transcription initiation site (Figure 5B); however, the peak position of the Smad3 binding was slightly different from that of Smad2. Notably, Smad3 binding was strongly enhanced in *Smad2*$^{\Delta/\Delta}$ BMDCs, whereas Smad2 binding was promoted in *Smad3*$^{-/-}$ BMDCs after TGF-β treatment (Figure 5C), suggesting that the recruitment of Smad3 to the CNS1 region resulted in activation of *Tgfb1* transcription, whereas that of Smad2 inhibited transcription. Smad4 was mainly recruited the Smad2 binding sites (probably due to a high Smad2 protein expression in DCs) (Figure S5A). However, Re-ChIP assay indicated that the Smad2-Smad4 complex was also recruited to the same Smad3-Smad4 binding site.

We next investigated histone modifications that affect transcription (Figure 5D). After TGF-β stimulation, −196 to −113 of the CNS1 showed the strongest Smad3 binding and transcriptionally active histone modifications (AcH3, AcH4, and H3K4me3) in WT BMDCs. AcH3 modification was observed in this region in BMDCs after long stimulation with PGN (Figure S5B). This region exhibited more transcriptionally active

(C) Murine TGF-β1 promoter genomic sequence homology to that of human (Hu) and bovine (Bv) estimated by ECR Browser (http://ecrbrowser.dcode.org/). Highly conserved regions were designated as CNS1 and CNS2. Position of the third exon of *B9d2* is shown. Blue color means protein-coding region.

(D) Promoter-reporter assay. The indicated murine *Tgfb1* promoter reporter constructs were transfected into HEK293-TLR2 cells together with control β-gal reporter plasmid, and then cells were stimulated with or without 100 ng/ml PGN for 24 hr and luciferase activity was measured and normalized to β-gal activity (RLA/β-gal). The conserved AP-1 binding site within CNS2 is shown as a circle (−1403 to −1397).

(E) BMDCs were stimulated by 100 ng/ml LPS or PGN for 6 hr, and then the ChIP assay for the corresponding regions was performed with anti-c-Fos, c-Jun, and acetylated histone H3 (AcH3) Abs. Data were pooled from two independent experiments.

(F) TGF-β protein concentrations secreted from WT or c-*Fos*$^{\Delta/\Delta}$ BMDCs stimulated with LPS, PGN, or *C. butyricum* for 24 hr.

(G) ChIP assay was performed with AcH3 Ab for the AP-1 binding region (−1508 to −1291) using PGN-stimulated WT or *Fos*$^{-/-}$ BMDCs.

(H) *Tgfb1* and *Fos* mRNA contents in LPDCs isolated from WT or *Fos*$^{\Delta DC/\Delta DC}$ mice administrated with CB for 14 days. Each mRNA amount was normalized to *Hprt* (n = 3).

(I) The percentage of Foxp3$^+$ within the CD4$^+$ cells (left) and the percentage of Nrp1$^-$ cells within the Foxp3$^+$CD4$^+$ cells (right) in the colonic LP of the indicated mice (n = 3).

All data represent the mean ± SEM (n = 3); *p < 0.05, **p < 0.01. Data were pooled from two independent experiments. See also Figure S3.

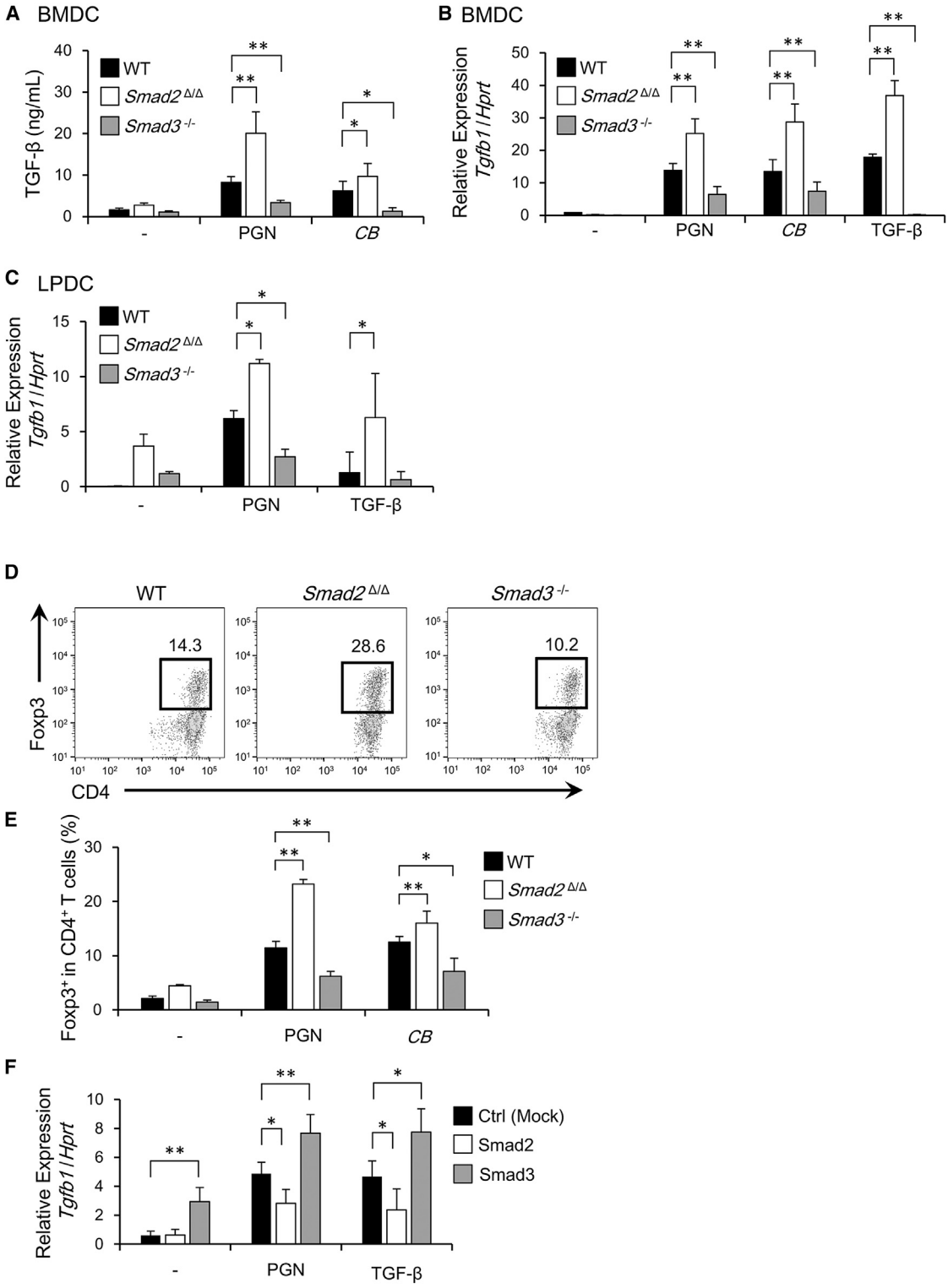

Figure 4. Opposing Roles of Smad2 and Smad3 in Autoinduction of TGF-β in DCs

(A) TGF-β secretion from WT, *Smad2*$^{\Delta/\Delta}$, and *Smad3*$^{-/-}$ BMDCs. BMDCs (1×10^6) were stimulated with 100 ng/ml PGN or 1×10^7 heat-killed *C. butyricum* (CB) for 24 hr and total TGF-β concentrations were determined by the SEAP assay.

(B) *Tgfb1* mRNA were normalized to *Hprt* in WT, *Smad2*$^{\Delta/\Delta}$, and *Smad3*$^{-/-}$ BMDCs stimulated with PGN, *C. butyricum*, or 5 ng/ml TGF-β for 3 hr.

(C) LPDCs isolated from WT, *Smad2*$^{\Delta/\Delta}$, and *Smad3*$^{-/-}$ mice were stimulated with 100 ng/ml PGN or 5 ng/ml TGF-β for 6 hr. Relative *Tgfb1* mRNA amounts normalized to *Hprt* are shown (n = 3).

(legend continued on next page)

histone modifications (AcH3, AcH4, and H3K4me3) and fewer repressive modifications (H3K9me3 and H3K27me3) in *Smad2*$^{\Delta/\Delta}$ BMDCs compared with WT BMDCs (Figure 5D). In contrast, *Smad3*$^{-/-}$ BMDCs showed lower active histone modifications than did WT BMDCs (Figure 5D). These data suggest that Smad3 induces active histone modifications, whereas Smad2 induces repressive ones.

To confirm this, we examined recruitment of histone acetyltransferase (HAT) p300 to the *Tgfb1* promoter (Figure 5E). Consistent with histone acetylation data (Figure 5D), many more p300 molecules were recruited to the CNS1 region in *Smad2*$^{\Delta/\Delta}$ BMDCs than in WT BMDCs, whereas p300 recruitment was severely reduced in *Smad3*$^{-/-}$ BMDCs (Figure 5E). It has been reported that Smad3-p300 interaction is required for Smad3-dependent transcription (Feng et al., 1998; Janknecht et al., 1998). Consistent with these reports, p300 was bound only to Smad3 (not to Smad2 and Smad4) in HEK293T cells (Figure S5C). Thus, Smad3 but not Smad2 recruits p300 to the CNS1 region, thereby promoting active histone modification and leading to *Tgfb1* transcription. On the other hand, a repressive histone modification, H3K9me3, was enhanced in *Smad3*$^{-/-}$ BMDCs (Figure 5D), suggesting that Smad2 might recruit H3K9 methyltransferases to the *Tgfb1* promoter.

Smad2-Deficient DCs Are Tolerogenic

Because *Smad2*$^{\Delta/\Delta}$ BMDCs expressed higher TGF-β and induced more iTreg cells in vitro compared with WT BMDCs, we investigated the effect of Smad2 deficiency in DCs in vivo. Colonic LP CD4$^+$ T cells contained higher fraction of Foxp3$^+$ Treg cells in *Smad2*$^{\Delta DC/\Delta DC}$ mice compared with WT mice under our specific-pathogen-free (SPF) conditions (Figures 6A and 6B). No significant difference in iTreg cells was observed in mLN between WT and *Smad2*$^{\Delta DC/\Delta DC}$ mice. The development of colonic CD11b$^+$CD103$^+$, CD11b$^-$CD103$^+$, and CD11b$^+$CD103$^-$ DCs was normal in *Smad2*$^{\Delta DC/\Delta DC}$ mice (Figures S6A and S6B); however, *Tgfb1* mRNA content in LPDCs from *Smad2*$^{\Delta DC/\Delta DC}$ mice was higher than those from WT mice (Figure 6C).

Administration of antibiotics resulted in reduced colonic Treg cell fraction in *Smad2*$^{\Delta DC/\Delta DC}$ mice compared to that in WT mice (Figures 6A and 6B), indicating that the enhanced Treg cell development in *Smad2*$^{\Delta DC/\Delta DC}$ mice was dependent on intestinal bacterial flora. Consistent with the increase of Treg cells in the colon of *Smad2*$^{\Delta DC/\Delta DC}$ mice, *Smad2*$^{\Delta DC/\Delta DC}$ mice were resistant to DSS-induced colitis (Figures 6D, S6C, and S6D). Expression of IL-10 and TGF-β1 increased in LPDCs of DSS-treated *Smad2*$^{\Delta DC/\Delta DC}$ mice compared with WT mice, whereas expression of inflammatory cytokines including TNF-α, IL-6, and IL-12p40 was decreased (Figure 6E). In addition, the IFN-γ$^+$ fraction in CD4$^+$ T cells was lower, whereas the Foxp3$^+$ fraction was higher in the LP of *Smad2*$^{\Delta DC/\Delta DC}$ mice than in WT mice after DSS treatment (Figure 6F).

Next, we investigated whether Smad2-deficient BMDCs were tolerogenic in vivo. PGN-treated *Smad2*$^{\Delta/\Delta}$ BMDCs produced high amount of TGF-β (Figure 4A); however, they expressed lower CD86, class II major histocompatibility complex (MHC) glycoproteins, and inflammatory cytokines than WT BMDCs (Figures 7A–7C), which are characteristic in tolerogenic DCs. We adoptively transferred *Smad2*$^{\Delta/\Delta}$ or WT BMDCs into *Rag2*$^{-/-}$ mice together with naive T cells. Transfer of naive T cells into *Rag2*$^{-/-}$ mice resulted in the development of fatal colitis. Co-transfer of WT BMDCs exacerbated colitis, whereas *Smad2*$^{\Delta/\Delta}$ BMDCs ameliorated colitis and reduced mortality (Figures 7D and 7E). WT BMDC transfer slightly increased LP IFN-γ$^+$CD4$^+$ T cells, whereas *Smad2*$^{\Delta/\Delta}$ BMDCs decreased IFN-γ$^+$ cells (Figure S7A). *Smad2*$^{\Delta/\Delta}$ BMDC transfer, highly increased Foxp3$^+$ cells in the colon, which was restored by the treatment with anti-TGF-β Ab (Figure 7F). A similar protective effect of *Smad2*$^{\Delta/\Delta}$ BMDCs was observed in a DSS-induced colitis model (Figures S7B and S7C). In this model, transfer of *Smad3*$^{-/-}$ BMDCs rather deteriorated colitis.

DISCUSSION

TGF-β is a pleiotropic cytokine that plays an essential role in immune homeostasis. One of the important functions of TGF-β for immune regulation is the induction of Foxp3$^+$ Treg cells, which are called iTreg or peripheral Treg (pTreg) cells. Various types of cells have been shown to secrete TGF-β, but the major producer for iTreg cell generation in the gut remains to be elucidated. LPDCs are the strongest candidate for iTreg cell generation in the colon; a number of reports attributed the major contribution of local iTreg cell accumulation to LPDCs (Benson et al., 2007; Coombes et al., 2007; Ruane and Lavelle, 2011; Sun et al., 2007). Indeed, we found that LPDCs produced much higher amounts of TGF-β in response to *C. butyricum* than epithelial cells.

LPDC populations have been shown to contain two distinct subsets: CD103$^+$CX$_3$CR1$^-$ LPDCs developed from pre-cDCs through a Flt3L growth-factor-mediated pathway and CD11b$^+$CD14$^+$CX$_3$CR1$^+$ LPDCs derived from Ly6C^{hi} monocytes under the control of granulocyte monocyte-colony stimulating factor (GM-CSF) (Varol et al., 2009). We have shown here that the CD103$^+$CX$_3$CR1$^-$ LPDC population most highly produced TGF-β in response to *C. butyricum*, which is consistent with the report showing that CD103$^+$ LPDCs suppress DSS-induced colitis (Varol et al., 2009). Although BMDCs were generated by GM-CSF, *Smad2*$^{-/-}$ BMDCs had tolerogenic potential with a high TGF-β expression. Further biochemical characterization of the TGF-β signaling might uncover a new mechanism of tolerogenic potential of CD103$^+$ LPDCs.

An increasing amount of evidence demonstrates a tight link between intestinal microbiota and local and systemic immune regulation including modification of helper T cell development.

(D and E) iTreg cell induction by *Smad2*$^{\Delta/\Delta}$ or *Smad3*$^{-/-}$ BMDCs. BALB/c naive CD4$^+$ T cells were cocultured for 3 days with the indicated genotype BMDCs, which were primed with PGN or *C. butyricum* for 24 hr. Foxp3$^+$ and CD4$^+$ T cell were analyzed by flow cytometry (D). The percentage of Foxp3$^+$ cells among CD4$^+$ T cells are shown quantitatively in (E). Data represent the mean ± SEM (n = 5). *p < 0.05, **p < 0.01.

(F) BMDCs infected with the retrovirus carrying Smad2 or Smad3 were stimulated by 100 ng/ml LPS, 100 ng/ml PGN, or 5 ng/ml TGF-β for 3 hr. *Tgfb1* mRNA was normalized to *Hprt*. Data represent the mean ± SEM (n = 3).

*p < 0.05, **p < 0.01. Data are representative of three independent experiments. See also Figure S4.

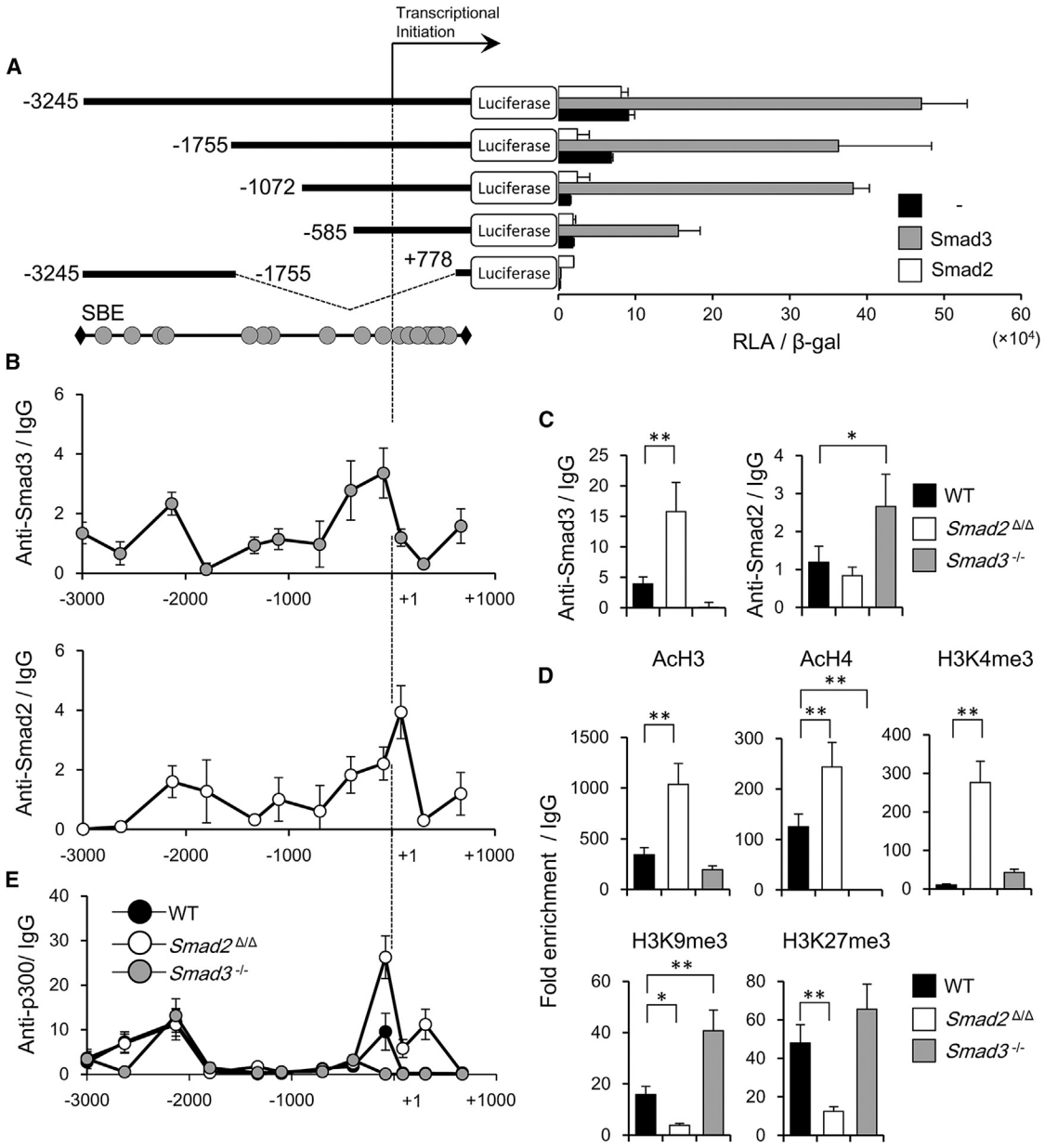

Figure 5. Smad2 and Smad3 Induce Distinctive Histone Modifications on the *Tgfb1* Promoter

(A) Smad-responsive region on the *Tgfb1* promoter. The indicated reporter plasmids were transfected into HEK293T cells together with Smad2 or Smad3 expression vectors. Luciferase activity in the cell lysates was measured and normalized to β-gal activity. Positions of the core SBE are shown as circles.

(B) WT BMDCs were stimulated with 5 ng/ml TGF-β for 6 hr, and then ChIP assay for indicated regions was performed with anti-Smad2 and anti-Smad3 Abs. n = 3 for each point.

(C) WT, *Smad2*$^{\Delta/\Delta}$, and *Smad3*$^{-/-}$ BMDCs were stimulated with TGF-β, and the ChIP assay for −196 to −113 region was performed with anti-Smad2 and Smad3 Abs.

(D) Histone modifications in WT, *Smad2*$^{\Delta/\Delta}$, and *Smad3*$^{-/-}$ BMDCs stimulated with TGF-β. The ChIP assay for the −196 to −113 region was performed with the indicated Abs.

(E) The ChIP assay with anti-p300 Ab for the indicated regions in WT, *Smad2*$^{\Delta/\Delta}$, and *Smad3*$^{-/-}$ BMDCs stimulated with TGF-β.

All data present the mean ± SEM (n = 3). *p < 0.05, **p < 0.01. Data were pooled from three independent experiments. See also Figure S5.

Treg cells are present at higher populations in the gut LP than in the other organs, and 1/2 to 2/3 of gut LP Treg cells are iTreg cells, which are probably dependent on TGF-β (Josefowicz et al., 2012). We showed here that intake of the gram-positive organism *C. butyricum* enhanced colonic LP iTreg cell development under normal feeding conditions, leading to resistance to DSS-induced colitis. Similarly, it has been reported that administration of probiotic strains of bifidobacteria and lactobacilli suppress colitis by inducing Treg cells in mice (Di Giacinto et al., 2005; Karimi et al., 2009; Lyons et al., 2010), and human

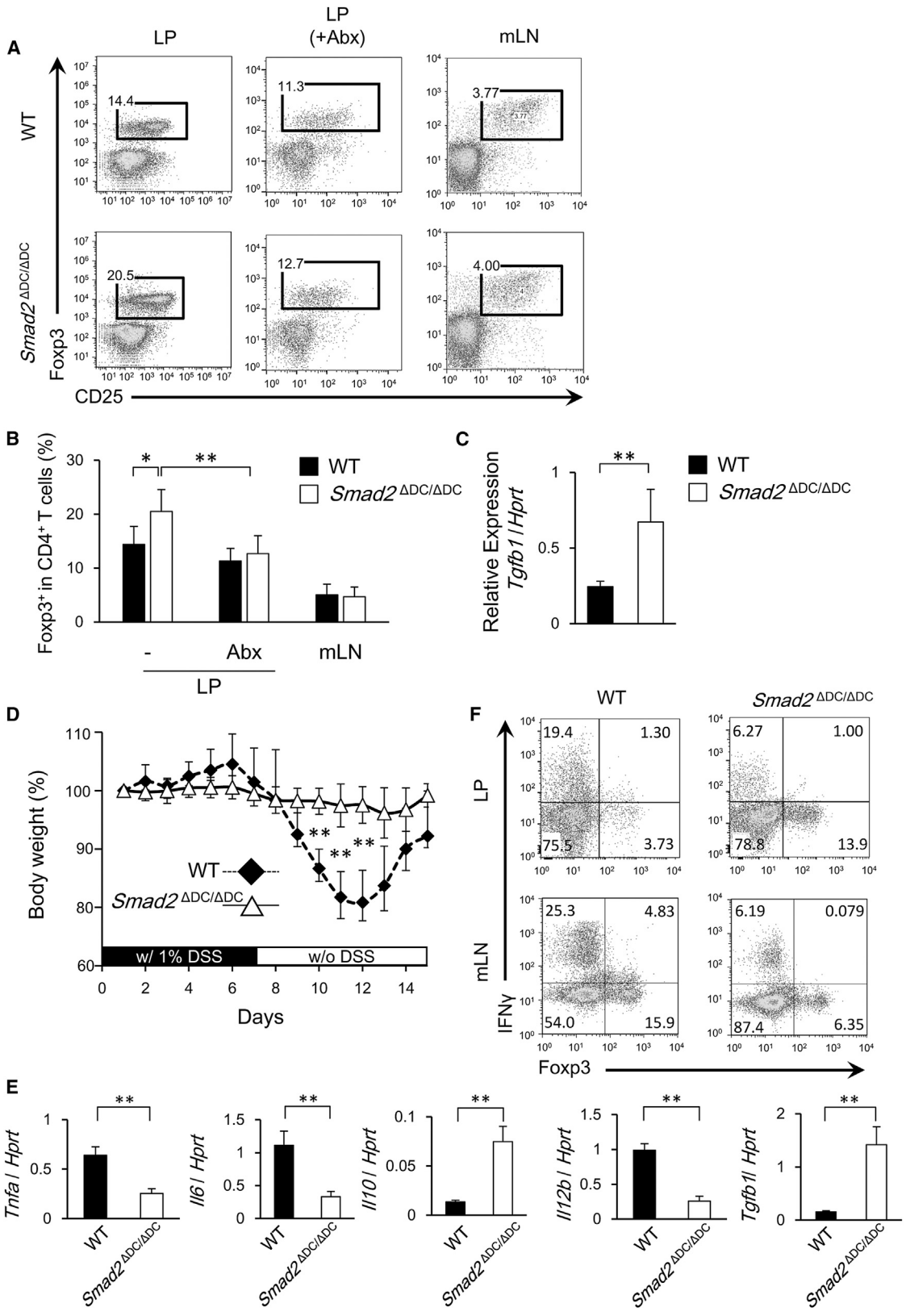

Figure 6. *Smad2*$^{\Delta DC/\Delta DC}$ Mice Show Higher Fractions of Intestinal iTreg Cells and Are More Resistant to DSS-Induced Colitis than WT Mice

(A and B) Treg cell population in the LP or mLN of *Smad2*$^{\Delta DC/\Delta DC}$ mice. Mice were maintained under SPF conditions or treated with antibiotics (Abx) for 14 days. Mononuclear cells from colonic LP or mLN were stained with anti-CD4, anti-CD25, and anti-Foxp3 Abs and analyzed with a flow cytometer. Representative flow

(legend continued on next page)

commensal *Bacteroides fragilis* facilitates Treg cell differentiation and IL-10 induction, thereby suppressing experimental autoimmune encephalomyelitis (Ochoa-Repáraz et al., 2010; Round and Mazmanian, 2010). Therefore, both IL-10 and Treg cell induction are involved in the effect of probiotic bacteria on immune regulation.

Induction of iTreg cells by *C. butyricum* is consistent with recent reports showing a preferential induction of Treg cells by murine and human *Clostridium* species (Atarashi et al., 2011, 2013). However, it is still unclear why particular *Clostridium* species specifically enhance iTreg cell generation. We showed that TLR-mediated ERK-AP-1 activation was an early event to activate the*Tgfb1* promoter and confirmed that TLR2 ligands activated AP-1 more strongly than TLR4 ligands. Therefore, preferential activation of TLR2 by *Clostridia* could be one mechanism. However, not all gram-positive bacteria promote iTreg cell development in mice. One possibility is that the different bacterial species produce different metabolites, because they produce different short chain fatty acids as described recently (Arpaia et al., 2013; Furusawa et al., 2013). Particular bacterial components might be involved, for example, a symbiosis factor (PSA, polysaccharide A) of *B. fragilis* promotes iTreg cell generation through TLR2 expression on Treg cells (Round et al., 2011) or DCs (Shen et al., 2012). Another possible mechanism is that DCs express distinctive cytokine patterns in response to different bacterial species.

Our study revealed a sequential mechanism of TGF-β1 production in DCs though AP-1 and Smad3. The role of AP-1 on *Tgfb1* expression has been reported in tumor cells (Birchenall-Roberts et al., 1990) and hepatocytes (Presser et al., 2013). However, AP-1 sites proposed in these studies located within the proximal region of the *Tgfb1* promoter and were not conserved between human and mouse. Neither study examined the distal region of the promoter including the AP-1 site we identified (−1403 to −1397). We also demonstrated autocrine activation of the *Tgfb1* promoter by Smad3. Previously, TGF-β-mediated *Tgfb1* promoter activation was reported in human lung adenocarcinoma cells, although the contribution of Smads was not considered (Kim et al., 1990). One paper suggested the involvement of Smad3 (Sato et al., 2003), but the Smad-binding region has not been identified. In addition, signals other than AP-1 might also play a role in the *Tgfb1* promoter activation. Indeed, we observed that a p38 inhibitor strongly suppressed *Tgfb1* expression in BMDCs, although we have not identified the transcription factor downstream of p38. We also showed that STAT3 is involved in the activation of the *Tgfb1* promoter in T cells (Kinjyo et al., 2006). It is possible that cell-type-specific transcription factors and signals might regulate TGF-β1 gene expression.

Another novel finding of our study is the negative role of Smad2 in TGF-β production in DCs. In T cells, we have shown that most of the TGF-β-induced or -repressed genes are redundantly regulated by Smad2 and Smad3 (Takimoto et al., 2010). For example, Smad2 and Smad3 are redundantly essential for Foxp3 induction (Takimoto et al., 2010), IL-9 expression (Tamiya et al., 2013), and IL-2 suppression (Wakabayashi et al., 2011) by TGF-β in T cells. Similarly, both Smad2 and Smad3 are important for the suppression of *Nos2* expression in macrophages (Sugiyama et al., 2012). Thus, *Tgfb1* is a rare gene which is oppositely regulated by Smad2 and Smad3. We propose that recruitment of p300 by Smad3 to the *Tgfb1* promoter is important because Smad2 does not bind to p300. Therefore, simple competition between active Smad3-Smad4 complex and silent Smad2-Smad4 complex to the Smad binding sites in the promoter might explain the opposite functions. Smad2 might also recruit transcription-repressive H3K9 methyltransferases to the *Tgfb1* promoter as observed in the *Il2* promoter (Wakabayashi et al., 2011).

We showed a strong tolerogenic potential of *Smad2*$^{\Delta/\Delta}$ DCs. TGF-β signals in DCs must play essential roles in generating tolerogenic DCs. In addition to TGF-β expression, tolerogenic DCs should express low amount of co-stimulators, class II MHCs, and inflammatory cytokines such as IL-12. Smad2 deficiency confers all the phenotypes necessary for Treg-cell-inducing tolerogenic DCs. We previously reported that, like *Smad2*$^{\Delta/\Delta}$ DCs, *Socs3*-deficient DCs showed similar tolerogenic phenotypes, namely, high TGF-β production and strong iTreg cell induction potential (Matsumura et al., 2007). In this case, higher STAT3 activation could be involved in the tolerogenic features of *Socs3*-deficient DCs, suggesting a cooperation of STAT3 and Smad3 for tolerogenicity in DCs. Specific inhibition of *Smad2* or *Socs3* expression by siRNA or gene editing methods might facilitate generation of tolerogenic DCs.

EXPERIMENTAL PROCEDURES

Mice

All mice used in this study were a C57BL/6 background. *Tlr2*$^{-/-}$, *Tlr4*$^{-/-}$, and *Tlr2*$^{-/-}$*Ttlr4*$^{-/-}$ mice were provided by Dr. S. Akira (Osaka University) and Dr. K. Miyake (Tokyo University). Mice with DC-specific *Smad2* deletion (*Itgax-cre-Smad2*$^{flox/flox}$) were generated by crossing *Itgax-cre* transgenic mice (Jackson Laboratory) and *Smad2*$^{flox/flox}$ mice (Ichiyama et al., 2011). *Smad3*$^{-/-}$ mice were provided by Dr. S. Saika (Wakayama Medical School). DC-specific *Fos*$^{-/-}$ (*Itgax-cre-Fos*$^{flox/flox}$) mice will be described elsewhere. All mice were housed in clean animal rooms under SPF conditions. All experiments with these mice were approved by and performed according to the guidelines of the animal ethics committee of Keio University, Tokyo, Japan. See Supplemental Experimental Procedures for colitis models, anti-TGF-β Ab treatment, and colonic cell preparation and flow cytometry analysis.

Bacteria Preparation

Clostridium butyricum MIYAIRI 588 (*C. butyricum*) used in this study was obtained from Miyarisan Pharmaceutical, as described (Hayashi et al., 2013). A gram-negative nonpathogenic strain of *E. coli* (25922; American Type Culture Collection) was cultured in Luria-Bertani medium. Bacteria were harvested and

cytometry profiles of CD25$^+$ and Foxp3$^+$ cells in the CD4$^+$ T cell fraction are shown in (A). Quantitative analysis of the percentage of Foxp3$^+$ Treg cells among CD4$^+$ T cells in (B) (n = 5).

(C) *Tgfb1* mRNA amounts were measured with qRT-PCR in LPDCs isolated from WT or *Smad2*$^{\Delta DC/\Delta DC}$ mice under normal diet conditions.

(D–F) DSS-induced colitis in WT and *Smad2*$^{\Delta DC/\Delta DC}$ mice. Body weight change of mice treated with and without 1.0% DSS for indicated periods (D). Cytokine amounts of LPDCs isolated from DSS-treated WT or *Smad2*$^{\Delta DC/\Delta DC}$ mice were measured with qRT-PCR (n = 5). (E) IFN-γ and Foxp3 staining in CD4$^+$ T cells isolated from LP or mLN of WT and *Smad2*$^{\Delta DC/\Delta DC}$ mice on day 8. Representative data of three independent experiments are shown (F).

*p < 0.05, **p < 0.01. See also Figure S6.

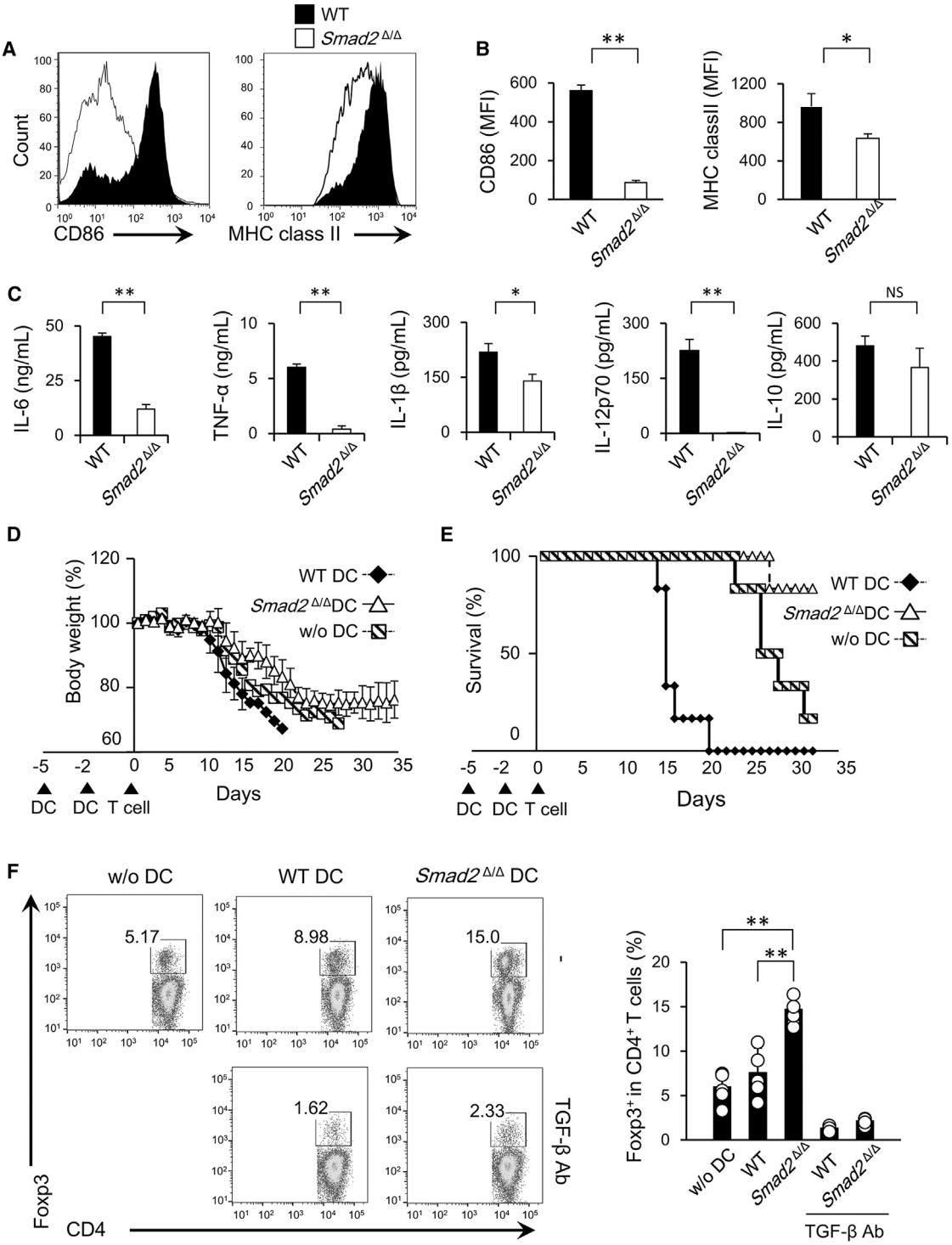

Figure 7. Tolerogenic Potential of *Smad2*-Deficient BMDCs

(A–C) BMDCs from WT or *Smad2*$^{\Delta DC/\Delta DC}$ mice were stimulated with 100 ng/ml PGN for 24 hr. BMDCs were stained with anti-CD86 and MHC class II (I-A^{b}) Abs and analyzed with flow cytometry (A) and quantified in (B). Cytokine concentrations in the culture of BMDCs from WT or *Smad2*$^{\Delta DC/\Delta DC}$ mice were determined with ELISA (C). Data are presented as the mean ± SEMs (n = 5). Data are representative of three independent experiments.

(D–F) Effect of WT and *Smad2*$^{\Delta/\Delta}$ BMDCs on colitis of *Rag2*$^{-/-}$ mice adoptively transferred with CD4^{+}CD62L^{hi} naive T cells. PGN-primed BMDCs (1 × 10^{6} cells) were transferred into *Rag2*$^{-/-}$ mice on day −2 and day −5 before transferring naive T cells. Changes in body weight (D) and survival (E) were measured daily (n = 8

(legend continued on next page)

washed twice with ice-cold PBS. Mice were fed with a diet containing 1×10^9 colony-forming units/g *C. butyricum* spore for 2 weeks as described (Hayashi et al., 2013). For heat-killed bacteria preparations, bacterial suspensions were boiled for 30 min, washed, re-suspended in PBS, and stored at −80°C until use.

Antibodies and Reagents

See Supplemental Experimental Procedures for antibodies, reagents, and biochemical assays.

Measurement of TGF-β

The TGF-β concentration was determined by bioassay with MFB-F11 cells as described (Matsumura et al., 2007). See Supplemental Experimental Procedures for Secreted Alkaline Phosphatase (SEAP) assay.

BMDC Preparation and MLR

BMDCs were prepared from bone marrow suspensions from femurs and tibias in mice as described (Matsumura et al., 2007). See Supplemental Experimental Procedures for isolation of native T cells and MLR.

mRNA Preparation and Quantitative RT-PCR

Total RNA was extracted with RNAiso Plus (TAKARA BIO) and subjected to reverse transcription with a High Capacity cDNA Synthesis Kit (Applied Biosystems). PCR analysis was performed with an iCycler iQ multicolor real-time PCR detection system (Bio-Rad) and SsoFast EvaGreen Supermix (Bio-Rad) with the indicated primer sets in Table S1. Relative expression levels were normalized to *Hprt*.

Chromatin Immunoprecipitation Assay

A ChIP assay for various transcription factors was performed as described previously (Tamiya et al., 2013). In brief, BMDCs were fixed with 1% formaldehyde at room temperature for 60 min and then suspended in an SDS lysis buffer. After sonication by the S220 Forcused-ultrasonicator (Covaris), samples were incubated with 2 μg antibodies or control IgG for 4 hr at 4°C. After the addition of Dynabeads protein G (Life Technologies), the immunoprecipitates were sequentially washed once each with a low-salt buffer, a high-salt buffer, a LiCl buffer, and twice with a TE buffer. The DNA-protein complex was eluted by heating at 65°C overnight. Proteins were then digested with proteinase K. DNA was recovered with the QIAquick PCR Purification Kit (QIAGEN) and then subjected to real-time PCR analysis. The primer sets are described in Table S2. See Supplemental Experimental Procedures for Re-ChIP assay.

Statistics

A paired, two-tailed Student's t test was used. Values of $p < 0.05$ were considered significant. All error bars represent the SEM.

SUPPLEMENTAL INFORMATION

Supplemental Information includes seven figures, two tables, and Supplemental Experimental Procedures and can be found with this article online at http://dx.doi.org/10.1016/j.immuni.2015.06.010.

AUTHOR CONTRIBUTIONS

I.K. performed experiments and wrote the manuscript. T.S. and T.K. advised the study and edited the manuscript and K.K., K.S., and A.H. performed experiments. M.M. and T.K. provided *Fos*$^{flox/flox}$ mice and M.N. provided *Smad2*$^{flox/flox}$ mice. A.Y. supervised the study and edited the manuscript.

ACKNOWLEDGMENTS

A.H. is supported by Miyarisan Pharmaceutical Co., Ltd. We thank M. Asakawa, S. Tsuruta, and R. Komine for technical assistance. This work was supported by special grants-in-aid from the Ministry of Education, Culture, Sports, Science and Technology of Japan, Intramural Research Grant (22-4) for Neurological and Psychiatric Disorders of National Center of Neurology and Psychiatry (NCNP), the SENSHIN Research Foundation, the Kanae Foundation for the Promotion of Medical Science, the Mochida Memorial Foundation, the Uehara Memorial Foundation, and the Takeda Science Foundation.

Received: September 2, 2014
Revised: March 3, 2015
Accepted: June 7, 2015
Published: June 30, 2015

REFERENCES

Agrawal, S., Agrawal, A., Doughty, B., Gerwitz, A., Blenis, J., Van Dyke, T., and Pulendran, B. (2003). Cutting edge: different Toll-like receptor agonists instruct dendritic cells to induce distinct Th responses via differential modulation of extracellular signal-regulated kinase-mitogen-activated protein kinase and c-Fos. J. Immunol. *171*, 4984–4989.

Arpaia, N., Campbell, C., Fan, X., Dikiy, S., van der Veeken, J., deRoos, P., Liu, H., Cross, J.R., Pfeffer, K., Coffer, P.J., and Rudensky, A.Y. (2013). Metabolites produced by commensal bacteria promote peripheral regulatory T-cell generation. Nature *504*, 451–455.

Atarashi, K., Tanoue, T., Shima, T., Imaoka, A., Kuwahara, T., Momose, Y., Cheng, G., Yamasaki, S., Saito, T., Ohba, Y., et al. (2011). Induction of colonic regulatory T cells by indigenous *Clostridium* species. Science *331*, 337–341.

Atarashi, K., Tanoue, T., Oshima, K., Suda, W., Nagano, Y., Nishikawa, H., Fukuda, S., Saito, T., Narushima, S., Hase, K., et al. (2013). Treg induction by a rationally selected mixture of Clostridia strains from the human microbiota. Nature *500*, 232–236.

Benson, M.J., Pino-Lagos, K., Rosemblatt, M., and Noelle, R.J. (2007). All-trans retinoic acid mediates enhanced T reg cell growth, differentiation, and gut homing in the face of high levels of co-stimulation. J. Exp. Med. *204*, 1765–1774.

Birchenall-Roberts, M.C., Ruscetti, F.W., Kasper, J., Lee, H.D., Friedman, R., Geiser, A., Sporn, M.B., Roberts, A.B., and Kim, S.J. (1990). Transcriptional regulation of the transforming growth factor beta 1 promoter by v-src gene products is mediated through the AP-1 complex. Mol. Cell. Biol. *10*, 4978–4983.

Chen, W., Jin, W., Hardegen, N., Lei, K.J., Li, L., Marinos, N., McGrady, G., and Wahl, S.M. (2003). Conversion of peripheral CD4+CD25- naive T cells to CD4+CD25+ regulatory T cells by TGF-beta induction of transcription factor Foxp3. J. Exp. Med. *198*, 1875–1886.

Coombes, J.L., and Powrie, F. (2008). Dendritic cells in intestinal immune regulation. Nat. Rev. Immunol. *8*, 435–446.

Coombes, J.L., Siddiqui, K.R., Arancibia-Cárcamo, C.V., Hall, J., Sun, C.M., Belkaid, Y., and Powrie, F. (2007). A functionally specialized population of mucosal CD103+ DCs induces Foxp3+ regulatory T cells via a TGF-beta and retinoic acid-dependent mechanism. J. Exp. Med. *204*, 1757–1764.

Di Giacinto, C., Marinaro, M., Sanchez, M., Strober, W., and Boirivant, M. (2005). Probiotics ameliorate recurrent Th1-mediated murine colitis by inducing IL-10 and IL-10-dependent TGF-beta-bearing regulatory cells. J. Immunol. *174*, 3237–3246.

Feng, X.H., Zhang, Y., Wu, R.Y., and Derynck, R. (1998). The tumor suppressor Smad4/DPC4 and transcriptional adaptor CBP/p300 are coactivators for smad3 in TGF-beta-induced transcriptional activation. Genes Dev. *12*, 2153–2163.

Furusawa, Y., Obata, Y., Fukuda, S., Endo, T.A., Nakato, G., Takahashi, D., Nakanishi, Y., Uetake, C., Kato, K., Kato, T., et al. (2013). Commensal

per group). *p < 0.05, **p < 0.01. (F) *Rag2*$^{-/-}$ mice were treated with or without TGF-β Ab on day −2 and day −5 when BMDCs were transferred. On day 14 after naive T cell transfer, Foxp3$^+$ cells in LP CD4$^+$ T cells were measured by intracellular flow cytometry staining. Representative flow cytometry profiles are shown in the left and the percentage of Foxp3$^+$ cells within CD4$^+$ cells are shown in the right (n = 5).
See also Figure S7.

microbe-derived butyrate induces the differentiation of colonic regulatory T cells. Nature *504*, 446–450.

Hayashi, A., Sato, T., Kamada, N., Mikami, Y., Matsuoka, K., Hisamatsu, T., Hibi, T., Roers, A., Yagita, H., Ohteki, T., et al. (2013). A single strain of *Clostridium butyricum* induces intestinal IL-10-producing macrophages to suppress acute experimental colitis in mice. Cell Host Microbe *13*, 711–722.

Hill, D.A., and Artis, D. (2010). Intestinal bacteria and the regulation of immune cell homeostasis. Annu. Rev. Immunol. *28*, 623–667.

Hooper, L.V., Littman, D.R., and Macpherson, A.J. (2012). Interactions between the microbiota and the immune system. Science *336*, 1268–1273.

Ichiyama, K., Sekiya, T., Inoue, N., Tamiya, T., Kashiwagi, I., Kimura, A., Morita, R., Muto, G., Shichita, T., Takahashi, R., and Yoshimura, A. (2011). Transcription factor Smad-independent T helper 17 cell induction by transforming-growth factor-β is mediated by suppression of eomesodermin. Immunity *34*, 741–754.

Ivanov, I.I., and Honda, K. (2012). Intestinal commensal microbes as immune modulators. Cell Host Microbe *12*, 496–508.

Janknecht, R., Wells, N.J., and Hunter, T. (1998). TGF-beta-stimulated cooperation of smad proteins with the coactivators CBP/p300. Genes Dev. *12*, 2114–2119.

Josefowicz, S.Z., Niec, R.E., Kim, H.Y., Treuting, P., Chinen, T., Zheng, Y., Umetsu, D.T., and Rudensky, A.Y. (2012). Extrathymically generated regulatory T cells control mucosal TH2 inflammation. Nature *482*, 395–399.

Karimi, K., Inman, M.D., Bienenstock, J., and Forsythe, P. (2009). *Lactobacillus reuteri*-induced regulatory T cells protect against an allergic airway response in mice. Am. J. Respir. Crit. Care Med. *179*, 186–193.

Kim, S.J., Angel, P., Lafyatis, R., Hattori, K., Kim, K.Y., Sporn, M.B., Karin, M., and Roberts, A.B. (1990). Autoinduction of transforming growth factor beta 1 is mediated by the AP-1 complex. Mol. Cell. Biol. *10*, 1492–1497.

Kinjyo, I., Inoue, H., Hamano, S., Fukuyama, S., Yoshimura, T., Koga, K., Takaki, H., Himeno, K., Takaesu, G., Kobayashi, T., and Yoshimura, A. (2006). Loss of SOCS3 in T helper cells resulted in reduced immune responses and hyperproduction of interleukin 10 and transforming growth factor-beta 1. J. Exp. Med. *203*, 1021–1031.

Lyons, A., O'Mahony, D., O'Brien, F., MacSharry, J., Sheil, B., Ceddia, M., Russell, W.M., Forsythe, P., Bienenstock, J., Kiely, B., et al. (2010). Bacterial strain-specific induction of Foxp3+ T regulatory cells is protective in murine allergy models. Clin. Exp. Allergy *40*, 811–819.

Massagué, J., Seoane, J., and Wotton, D. (2005). Smad transcription factors. Genes Dev. *19*, 2783–2810.

Matsumura, Y., Kobayashi, T., Ichiyama, K., Yoshida, R., Hashimoto, M., Takimoto, T., Tanaka, K., Chinen, T., Shichita, T., Wyss-Coray, T., et al. (2007). Selective expansion of foxp3-positive regulatory T cells and immunosuppression by suppressors of cytokine signaling 3-deficient dendritic cells. J. Immunol. *179*, 2170–2179.

Ochoa-Repáraz, J., Mielcarz, D.W., Wang, Y., Begum-Haque, S., Dasgupta, S., Kasper, D.L., and Kasper, L.H. (2010). A polysaccharide from the human commensal *Bacteroides fragilis* protects against CNS demyelinating disease. Mucosal Immunol. *3*, 487–495.

Ohnmacht, C., Pullner, A., King, S.B., Drexler, I., Meier, S., Brocker, T., and Voehringer, D. (2009). Constitutive ablation of dendritic cells breaks self-tolerance of CD4 T cells and results in spontaneous fatal autoimmunity. J. Exp. Med. *206*, 549–559.

Presser, L.D., McRae, S., and Waris, G. (2013). Activation of TGF-β1 promoter by hepatitis C virus-induced AP-1 and Sp1: role of TGF-β1 in hepatic stellate cell activation and invasion. PLoS ONE *8*, e56367.

Ramalingam, R., Larmonier, C.B., Thurston, R.D., Midura-Kiela, M.T., Zheng, S.G., Ghishan, F.K., and Kiela, P.R. (2012). Dendritic cell-specific disruption of TGF-β receptor II leads to altered regulatory T cell phenotype and spontaneous multiorgan autoimmunity. J. Immunol. *189*, 3878–3893.

Re, F., and Strominger, J.L. (2001). Toll-like receptor 2 (TLR2) and TLR4 differentially activate human dendritic cells. J. Biol. Chem. *276*, 37692–37699.

Round, J.L., and Mazmanian, S.K. (2010). Inducible Foxp3+ regulatory T-cell development by a commensal bacterium of the intestinal microbiota. Proc. Natl. Acad. Sci. USA *107*, 12204–12209.

Round, J.L., Lee, S.M., Li, J., Tran, G., Jabri, B., Chatila, T.A., and Mazmanian, S.K. (2011). The Toll-like receptor 2 pathway establishes colonization by a commensal of the human microbiota. Science *332*, 974–977.

Ruane, D.T., and Lavelle, E.C. (2011). The role of $CD103^+$ dendritic cells in the intestinal mucosal immune system. Front. Immunol. *2*, 25.

Sato, R., and Tanaka, M. (1997). Intestinal distribution and intraluminal localization of orally administered *Clostridium butyricum* in rats. Microbiol. Immunol. *41*, 665–671.

Sato, M., Muragaki, Y., Saika, S., Roberts, A.B., and Ooshima, A. (2003). Targeted disruption of TGF-beta1/Smad3 signaling protects against renal tubulointerstitial fibrosis induced by unilateral ureteral obstruction. J. Clin. Invest. *112*, 1486–1494.

Seki, H., Shiohara, M., Matsumura, T., Miyagawa, N., Tanaka, M., Komiyama, A., and Kurata, S. (2003). Prevention of antibiotic-associated diarrhea in children by *Clostridium butyricum* MIYAIRI. Pediatr. Int. *45*, 86–90.

Shen, Y., Giardino Torchia, M.L., Lawson, G.W., Karp, C.L., Ashwell, J.D., and Mazmanian, S.K. (2012). Outer membrane vesicles of a human commensal mediate immune regulation and disease protection. Cell Host Microbe *12*, 509–520.

Sugiyama, Y., Kakoi, K., Kimura, A., Takada, I., Kashiwagi, I., Wakabayashi, Y., Morita, R., Nomura, M., and Yoshimura, A. (2012). Smad2 and Smad3 are redundantly essential for the suppression of iNOS synthesis in macrophages by regulating IRF3 and STAT1 pathways. Int. Immunol. *24*, 253–265.

Sun, C.M., Hall, J.A., Blank, R.B., Bouladoux, N., Oukka, M., Mora, J.R., and Belkaid, Y. (2007). Small intestine lamina propria dendritic cells promote de novo generation of Foxp3 T reg cells via retinoic acid. J. Exp. Med. *204*, 1775–1785.

Takimoto, T., Wakabayashi, Y., Sekiya, T., Inoue, N., Morita, R., Ichiyama, K., Takahashi, R., Asakawa, M., Muto, G., Mori, T., et al. (2010). Smad2 and Smad3 are redundantly essential for the TGF-beta-mediated regulation of regulatory T plasticity and Th1 development. J. Immunol. *185*, 842–855.

Tamiya, T., Ichiyama, K., Kotani, H., Fukaya, T., Sekiya, T., Shichita, T., Honma, K., Yui, K., Matsuyama, T., Nakao, T., et al. (2013). Smad2/3 and IRF4 play a cooperative role in IL-9-producing T cell induction. J. Immunol. *191*, 2360–2371.

Varol, C., Vallon-Eberhard, A., Elinav, E., Aychek, T., Shapira, Y., Luche, H., Fehling, H.J., Hardt, W.D., Shakhar, G., and Jung, S. (2009). Intestinal lamina propria dendritic cell subsets have different origin and functions. Immunity *31*, 502–512.

Wakabayashi, Y., Tamiya, T., Takada, I., Fukaya, T., Sugiyama, Y., Inoue, N., Kimura, A., Morita, R., Kashiwagi, I., Takimoto, T., et al. (2011). Histone 3 lysine 9 (H3K9) methyltransferase recruitment to the interleukin-2 (IL-2) promoter is a mechanism of suppression of IL-2 transcription by the transforming growth factor-β-Smad pathway. J. Biol. Chem. *286*, 35456–35465.

Worthington, J.J., Czajkowska, B.I., Melton, A.C., and Travis, M.A. (2011). Intestinal dendritic cells specialize to activate transforming growth factor-β and induce Foxp3+ regulatory T cells via integrin αvβ8. Gastroenterology *141*, 1802–1812.

Yadav, M., Louvet, C., Davini, D., Gardner, J.M., Martinez-Llordella, M., Bailey-Bucktrout, S., Anthony, B.A., Sverdrup, F.M., Head, R., Kuster, D.J., et al. (2012). Neuropilin-1 distinguishes natural and inducible regulatory T cells among regulatory T cell subsets in vivo. J. Exp. Med. *209*, 1713–1722, S1–S19.